Supporting Information for "Attribution of the influence of human-induced climate change on an extreme fire season"

M. C. Kirchmeier-Young[1,2], N. P. Gillett[2], F. W. Zwiers[1], A. J. Cannon[3], F. S. Anslow[1]

[1] Pacific Climate Impacts Consortium, University of Victoria, Victoria BC V8W 2Y2, Canada
[2] Canadian Centre for Climate Modelling and Analysis, Environment and Climate Change Canada, Victoria BC V8W 2Y2, Canada
[3] Climate Research Division, Environment and Climate Change Canada, Victoria BC V8W 2Y2, Canada

Corresponding author: M. C. Kirchmeier-Young (megan.kirchmeier-young@canada.ca)

Contents of this file:

Text S1: Model Simulations

We utilized a large ensemble of the Canadian Regional Climate Model (CanRCM4; Scinocca et al. 2016). There are 50 realizations that are each driven by one of the 50 realizations from a large ensemble of the Canadian Earth System Model (CanESM2; Arora et al. 2011). The CanESM2 realizations use historical ALL forcing as defined by CMIP5 from 1950-2005 and RCP 8.5 continuing through 2100. The CanRCM4 large ensemble is run on the CORDEX (http://cordex.org) North American .44 degree (50 km) rotated pole grid. For more details on model specifications and the coordinated modeling approach, see Scinocca et al. (2016).

We used 3-hourly archived outputs for the period 1961-2020. Inputs for the CFFDRS calculations (air temperature, relative humidity, wind speed, precipitation) were taken at 21 UTC to approximate the local noon values requested by the CFFDRS routine and provided by the reanalysis dataset described below. Precipitation was calculated as a 24-hour accumulation prior to this time. All other variables (mean, maximum, and minimum air temperature, and snow depth) were taken from the daily outputs. Vapor pressure deficit was calculated using the daily air temperature, specific humidity, and surface pressure derived from the model-supplied sea level pressure.

Text S2: Reanalysis Dataset

The requirement for relative humidity and wind speed data limit the use of observation datasets and we instead utilize a reanalysis product. The Global Fire Weather Database (GFWED; Field et al. 2015) provides a dataset of the main CFFDRS indices and their input variables with global coverage on the MERRA2 reanalysis grid (1/2 degrees latitude x 2/3 degrees longitude). The input variables are local noon values taken from the MERRA2 reanalysis and multiple precipitation options are available. We utilized the air temperature, relative humidity, wind speed, and snow depth provided by GFWED. CFFDRS calculations were performed by the authors to ensure consistency with the calculations for the CanRCM4 simulations; see later section for more details.

Following Kirchmeier-Young et al. (2017), precipitation was taken from the Multi-Source Weighted-Ensemble Precipitation (MSWEP) dataset (Beck et al., 2017) version 1.6. In our region of interest, this dataset blends reanalyses and remotely-sensed observations, with additional input from surface station observations. Approximately local-noon to local-noon accumulations were calculated from the 3-hourly files and the MSWEP data were interpolated to the MERRA2 grid to match the GFWED. In the time series plots (Figs. 4, S3, S6), this dataset (referred to as MERRA2/MSWEP) is shown in turquoise covering 1980-2014. The MSWEP data were not available through 2017, so a second dataset was used when 2017 values were required. Here all variables were taken from the MERRA2 reanalysis and the precipitation was bias corrected (via quantile-mapping) towards the MSWEP dataset. This dataset is shown in purple and covers 1980-2017.

Values for daily mean, maximum, and minimum temperature were taken from the MERRA2 reanalysis and vapor pressure deficit was calculated using the reanalysis-supplied dew point temperature. The Southern Cordillera homogeneous fire regime zone (Boulanger et al., 2014) in British Columbia (BC) comprises 86 grid boxes for the MERRA2 reanalysis.

Text S3: Observations

Observations of fire locations and perimeters are available for public download (under the Open Government License – British Columbia) from the BC Wildfire Service through the BC Data Catalogue (`https://catalogue.data.gov.bc.ca`). To determine area burned totals for the SCBC region, intersections of each fire polygon and the BC Southern Cordillera polygon were calculated using the shapefiles in Python. Areas of each intersection polygon were calculated and summed by year. Fire counts for each year were determined by extracting fire incidents from a list of fire locations when the latitude/longitude point was within the BC Southern Cordillera region. Area burned totals calculated from the fire locations resulted in only minor differences from the values determined from the polygons. Restricting the homogeneous fire regime zone to BC allows for comparison to these provincial observations datasets.

A dataset of gridded maximum (and minimum) temperature and precipitation anomalies was created by interpolating monthly values calculated from surface station observations relative to 30 year climatology. Observational data were obtained from Environment and Climate Change Canada, British Columbia Ministries, the regional hydropower utility BC Hydro and RioTinto. Data for Alberta and Yukon Territory were obtained from Environment and Climate Change Canada and no observations from the US were incorporated. Data underwent nominal single station quality control tests and elimination that including range checking and consistency checks. Climatological averages for the 1981-2010 climate normal period were calculated in two steps. First, normals were calculated for records with more than twenty two years of data within the normal period. Second, additional normals were calculated for stations with shorter periods of record by computing the offset in average between the short period of record in common with the target station and the long-term average and then applying the average offset from three nearby long term stations to the short-term average. For calculating the time series of monthly averages/sums for each station, a requirement of 85% data availability for a monthly value to be calculated was imposed. Anomalies in temperature are simple differences between the observed value and the normal. For precipitation, anomalies were divided by the long term average to yield unitless normalized values suitable for interpolation. The station data were gridded by interpolating the anomalies for a given month, year and variable using all available stations. Interpolation was performed with thin plate splines within the R statistical software package "fields" with spline parameters optimized through minimization of the cross validation error. Covariates were not used in computing the spline. Data were interpolated to a grid with 0.5 degree latitude/longitude spacing covering all of British Columbia. Spline interpolation can suffer from non-physical overshoot errors if there are insufficient constraining data, but for the region, the season, and the period of interest, station density is high for all variables and years of analysis making overshooting unlikely.

For the detection and attribution analysis, the CRU TS3.23 dataset (Harris et al., 2014) of monthly mean air temperature anomalies was acquired. This dataset is available for land areas on a 0.5 degree grid. It provides the mean temperature anomalies not included in the BC station product described above and has the advantage over a reanalysis of being based on station observations.

Text S4: Bias Correction

The bias correction procedure applied to CanRCM4 is similar to that from Kirchmeier-Young et al. (2017) for CanESM2. The CanRCM4 realizations were interpolated to the MERRA2 grid over southern BC and a bias correction routine was applied. We used the n-dimensional Multivariate Bias Correction (MBCn) from Cannon (2018) and the reader is directed to the MBCn methods paper for technical details. In general, the MBCn framework applies a quantile-mapping bias correction technique to each variable, while maintaining the covariance structure between all input variables.

We bias correct together all variables needed for the analyses: mid-day air temperature, relative humidity, wind speed, and precipitation, and daily mean air temperature, maximum temperature, minimum temperature, mean vapor pressure deficit, and snow depth. The bias correction procedure was performed for each CanRCM4 realization. First, anomalies relative to the CanRCM4 1981-2010 climatology for each variable were calculated on the original model grid. Next, the anomalies were bi-linearly interpolated to the MERRA2 grid and the MERRA2/MSWEP climatology added. Finally, the quantile mapping was performed. The temperature variables used difference climatologies, while precipitation and wind speed used ratios. It was more stable to remap snow depth, vapor pressure deficit, and relative humidity using realized values instead of anomalies.

The bias correction was trained using 1980-2014, with the MERRA2/MSWEP dataset described above as the target. To apply the bias correction to the 50 CanRCM4 realizations (1961-2020), each realization received a mapping trained with a different realization in order to preserve the internal variability of the large ensemble.

Text S5: CFFDRS calculations

The Canadian Forest Fire Danger Rating System (CFFDRS; Wotton 2009) contains numerous indices that describe aspects of fire weather and behavior potential. All indices increase with increasing severity. The CFFDRS indices are calculated following the equations outlined in Van Wagner (1987) for the Fire Weather Index (FWI) System and Forestry Canada Fire Danger Group (1992) for the Fire Behavior Prediction (FBP) System. Calculations are performed daily and for each grid box separately. Standard initial values are used at the beginning of the fire season and for simplicity, we do not consider overwintering. FBP calculations are done using fuel type C-3 mature jack or lodgepole pine, which is the dominant fuel type in the BC Southern Cordillera region (Perrakis & Eade, 2016). Each year, the calculation of the indices begins after three consecutive days without snow cover or after three consecutive days with noon temperatures exceeding 12 °C, if there was insufficient winter snow cover (Kirchmeier-Young et al., 2017). As in Field et al. (2015) for GFWED, snow cover is defined by a snow depth exceeding 1 cm. The calculations cease, signaling the end of the fire season, on the first day (after 01 July) that has snow cover.

Text S6: Detection and Attribution

To investigate the anthropogenic influence on regional temperature in CanRCM4, a detection and attribution analysis was performed for annual and summer (JJA) anomalies averaged over BC (Fig. S1). A regression approach using regularized optimal fingerprinting (Ribes et al., 2013) was applied to the ensemble mean of CanRCM4 simulations (before bias correction) and observed temperature anomalies from the CRU TS3.23 dataset (Harris et al., 2014).

The detection and attribution methodology is similar to that used in Kirchmeier-Young et al. (2017) for CanESM2 for the one signal (all forcing) analysis, though the region and time period are slightly different. The covariance matrix to represent internal climate variability was constructed by differencing 49 (of the 50) realizations from the ensemble mean. Scaling factors greater than 0 indicate the all-forcing signal from the RCM is detected in the observations. A scaling factor consistent with 1.0 implies the observed and modeled signals are of the same amplitude, while smaller scaling factors indicate the modeled trend is greater than that from observations.

References

Amiro, B. D., Logan, K. A., Wotton, B. M., Flannigan, M. D., Todd, J. B., Stocks, B. J., & Martell, D. L. (2004). Fire weather index system componenets for large fires in the Canadian boreal forest. *International Journal of Wildland Fire*, *13*(4), 391–400. doi: 10.1071/WF03066

Arora, V. K., Scinocca, J. F., Boer, G. J., Christian, J. R., Denman, K. L., Flato, G. M., ... Merryfield, W. J. (2011, mar). Carbon emission limits required to satisfy future representative concentration pathways of greenhouse gases. *Geophysical Research Letters*, *38*, L05805. doi: 10.1029/2010GL046270

Beck, H. E., van Dijk, A. I. J. M., Levizzani, V., Schellekens, J., Miralles, D. G., Martens, B., & de Roo, A. (2017). MSWEP: 3-hourly 0.25 global gridded precipitation (1979-2015) by merging gauge, satellite, and reanalysis data. *Hydrology and Earth System Sciences*, *21*(1), 589–615. doi: 10.5194/hess-2016-236

Boulanger, Y., Gauthier, S., & Burton, P. J. (2014). A refinement of models projecting future Canadian fire regimes using homogeneous fire regime zones. *Canadian Journal of Forest Research*, *44*(4), 365–376. doi: 10.1139/cjfr-2013-0372

Cannon, A. J. (2018). Multivariate quantile mapping bias correction: An N-dimensional probability density function transform for climate model simulations of multiple variables. *Climate Dynamics*, *50*, 31–49. doi: 10.1007/s00382-017-3580-6

Field, R. D., Spessa, A. C., Aziz, N. A., Camia, A., Cantin, A., Carr, R., ... Wang, X. (2015). Development of a Global Fire Weather Database. *Natural Hazards and Earth System Sciences*, *15*, 1407–1423. doi: 10.5194/nhess-15-1407-2015

Forestry Canada Fire Danger Group. (1992). Development and Structure of the Canadian Forest Fire Behavior Predition System. In *Information report st-x-3* (p. 64). Ottawa.

Harris, I., Jones, P. D., Osborn, T. J., & Lister, D. H. (2014). Updated high-resolution grids of monthly climatic observations - the CRU TS3.10 Dataset. *International Journal of Climatology*, *34*, 623–642. doi: 10.1002/joc.3711

Kirchmeier-Young, M. C., Zwiers, F. W., Gillett, N. P., & Cannon, A. J. (2017). Attributing extreme fire risk in Western Canada to human emissions. *Climatic Change*, *144*, 365–379. doi: 10.1007/s10584-017-2030-0

Perrakis, D. D. B., & Eade, G. (2016). *British Columbia wildfire fuel typing and fuel type layer description* (Tech. Rep.). Victoria, British Columbia: BC Wildfire Service HQ, Ministry of Forests, Lands, and Natural Resource Operations.

Ribes, A., Planton, S., & Terray, L. (2013). Application of regularised optimal fingerprinting to attribution. Part I: method, properties and idealised analysis. *Climate Dynamics*, *41*, 2817–2836. doi: 10.1007/s00382-013-1735-7

Scinocca, J. F., Kharin, V. V., Jiao, Y., Qian, M. W., Lazare, M., Solheim, L., ... Dugas, B. (2016). Coordinated global and regional climate modeling. *Journal of Climate*, *29*(1), 17–35. doi: 10.1175/JCLI-D-15-0161.1

Van Wagner, C. E. (1987). *Development and structure of the Canadian Fire Weather Index System* (Vol. 35). Ottawa: Canadian Forestry Service. doi: 19927

Wotton, B. M. (2009). Interpreting and using outputs from the Canadian Forest Fire Danger Rating System in research applications. *Environmental and Ecological Statistics*, *16*(2), 107–131. doi: 10.1007/s10651-007-0084-2

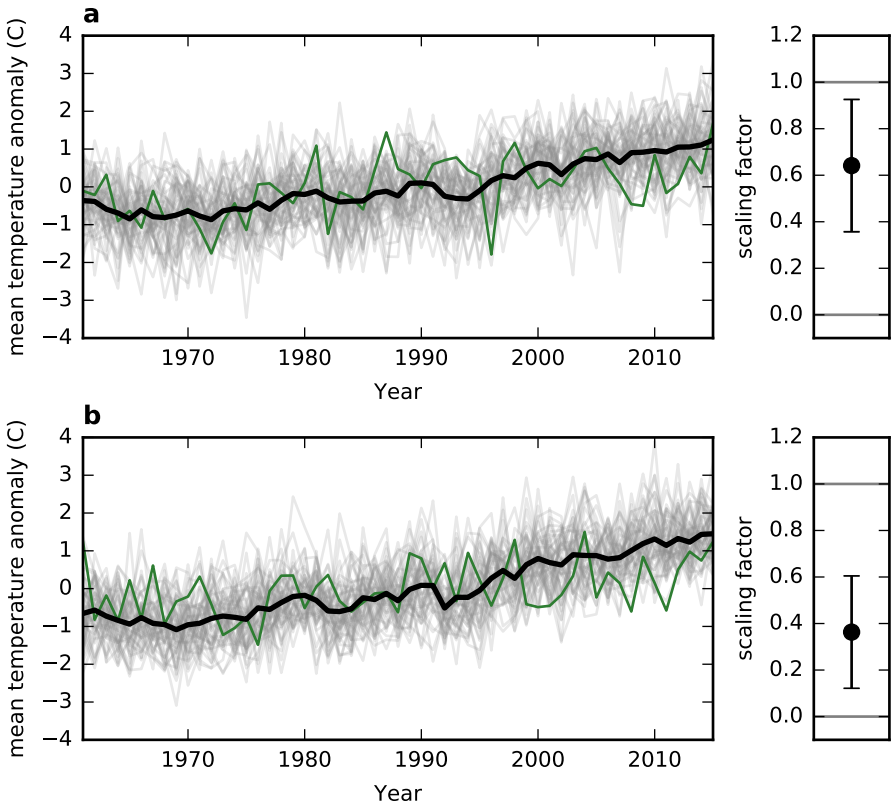

Figure S1: Detection and attribution results using CanRCM4 and observations from CRU-TS3.23 for annual mean temperature anomalies (a) and summer (JJA) mean temperature anomalies (b) averaged over British Columbia. Time series on the left are shown for each CanRCM4 realization (pre-bias correction) in grey, with the ensemble mean in bold black and the observations in green. Anomalies are calculated relative to the entire period shown. Using the 1961-2015 period, scaling factors (plotted on the right with 90% confidence intervals) were determined using a one-signal analysis comparing the all-forcing simulations with the observed pattern.

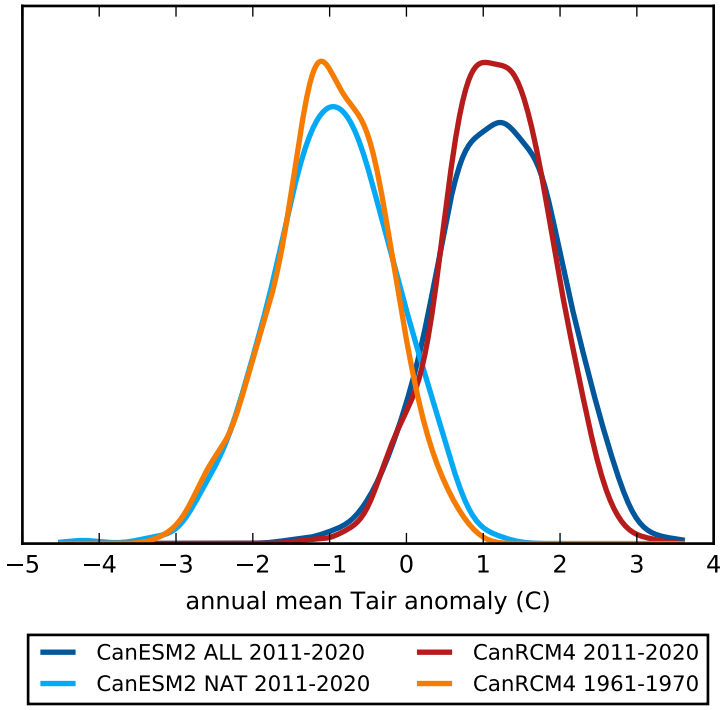

Figure S2: Comparison of chosen decades of CanRCM4 simulations with different forcing scenarios of the global model. Probability distributions of annual mean temperature anomalies estimated using Gaussian kernel densities are plotted for the late period for CanRCM4 (2011-2020; red) and the early period of CanRCM4 (1961-1970; orange), as well as for 2011-2020 using all forcing (through 2005) and RCP 8.5 (2006 onward) simulations from CanESM2 (dark blue) and natural-only forcing simulations from CanESM2 (light blue). Temperature anomalies are calculated for land grid boxes at each model's native resolution and averaged (with area weighting) over western Canada (latitudes between 48 and 70 degrees N and longitudes between -140 and -95 degrees E). Anomalies are relative to 1981-2010.

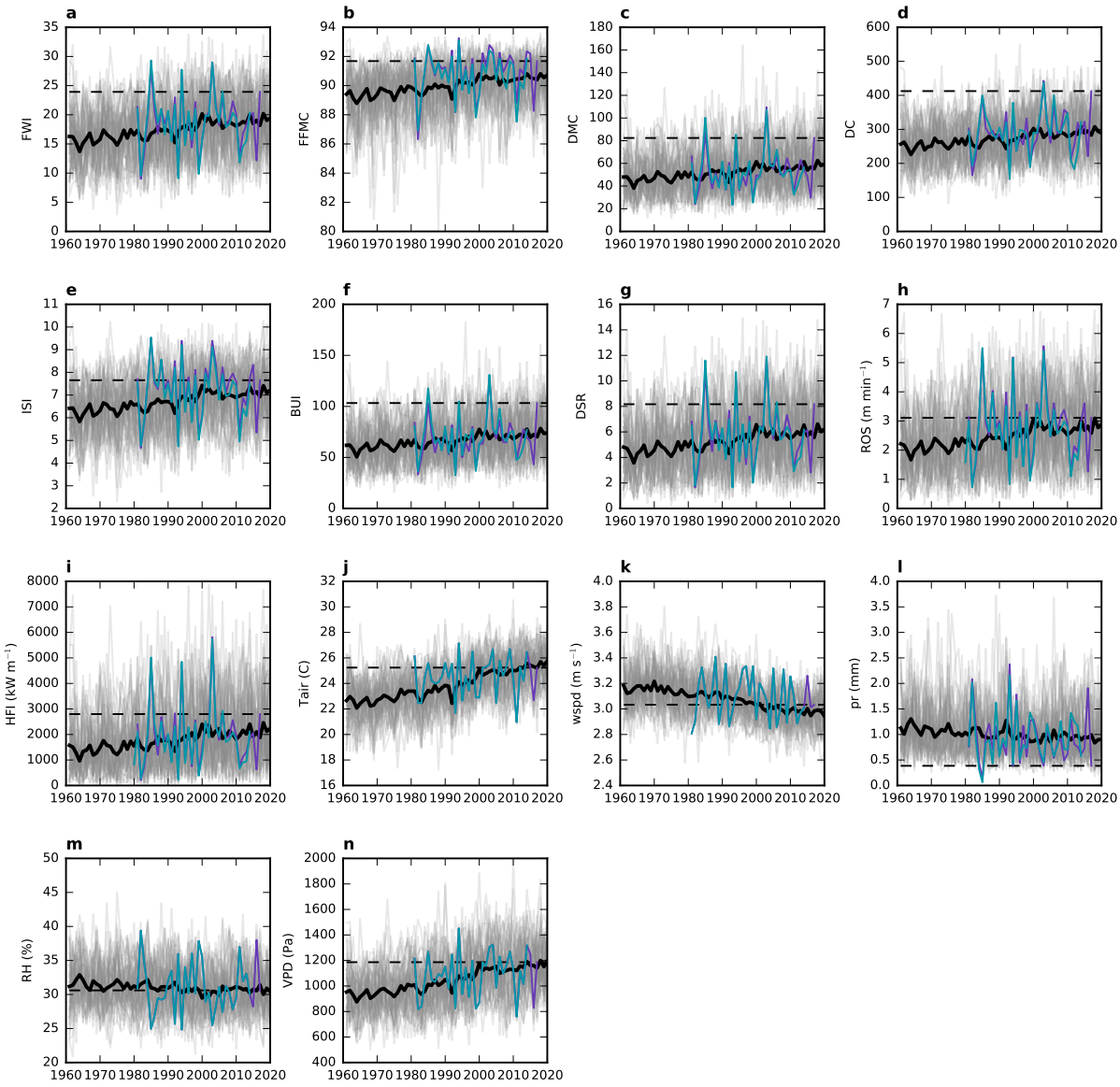

Figure S3: Time series of the annual July-August 95th percentile value of daily values of each CFFDRS index [FWI (a), FFMC (b), DMC (c), DC (d), ISI (e), BUI (f), DSR (g), ROS (h), HFI (i)] and input variable [Tair (j), wspd (k), pr (l), RH (m), VPD (n)] for each year averaged across SCBC are plotted in light grey for each model realization and in bold black for the ensemble mean. The values from the MERRA2/MSWEP dataset are plotted in purple and MERRA2 in turquoise. The 2017 value is identified with the horizontal dashed line. RH uses the 5th percentile and pr uses the 50th percentile.

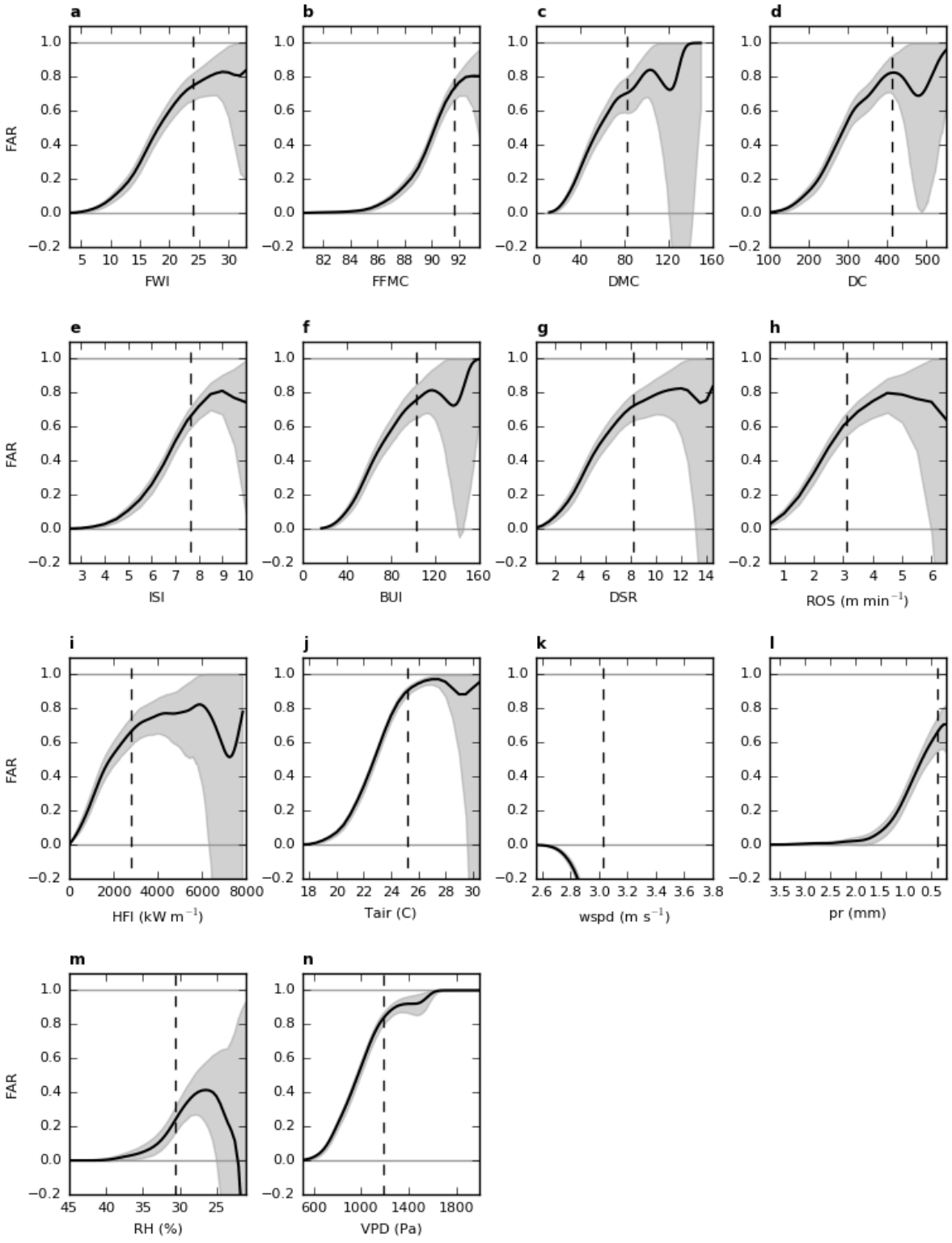

Figure S4: FAR values for the July-August 95th percentile value of each CFFDRS index [FWI (a), FFMC (b), DMC (c), DC (d), ISI (e), BUI (f), DSR (g), ROS (h), HFI (i)] and input variable [Tair (j), wspd (k), pr (l), RH (m), VPD (n)] averaged across the BC Southern Cordillera exceeding the threshold on the horizontal axis. The vertical dashed line represents the 2017 value used as the threshold in Fig. 3. The 90% confidence interval (shaded) was determined through bootstrapping. FAR values are plotted only over the range of realized values.

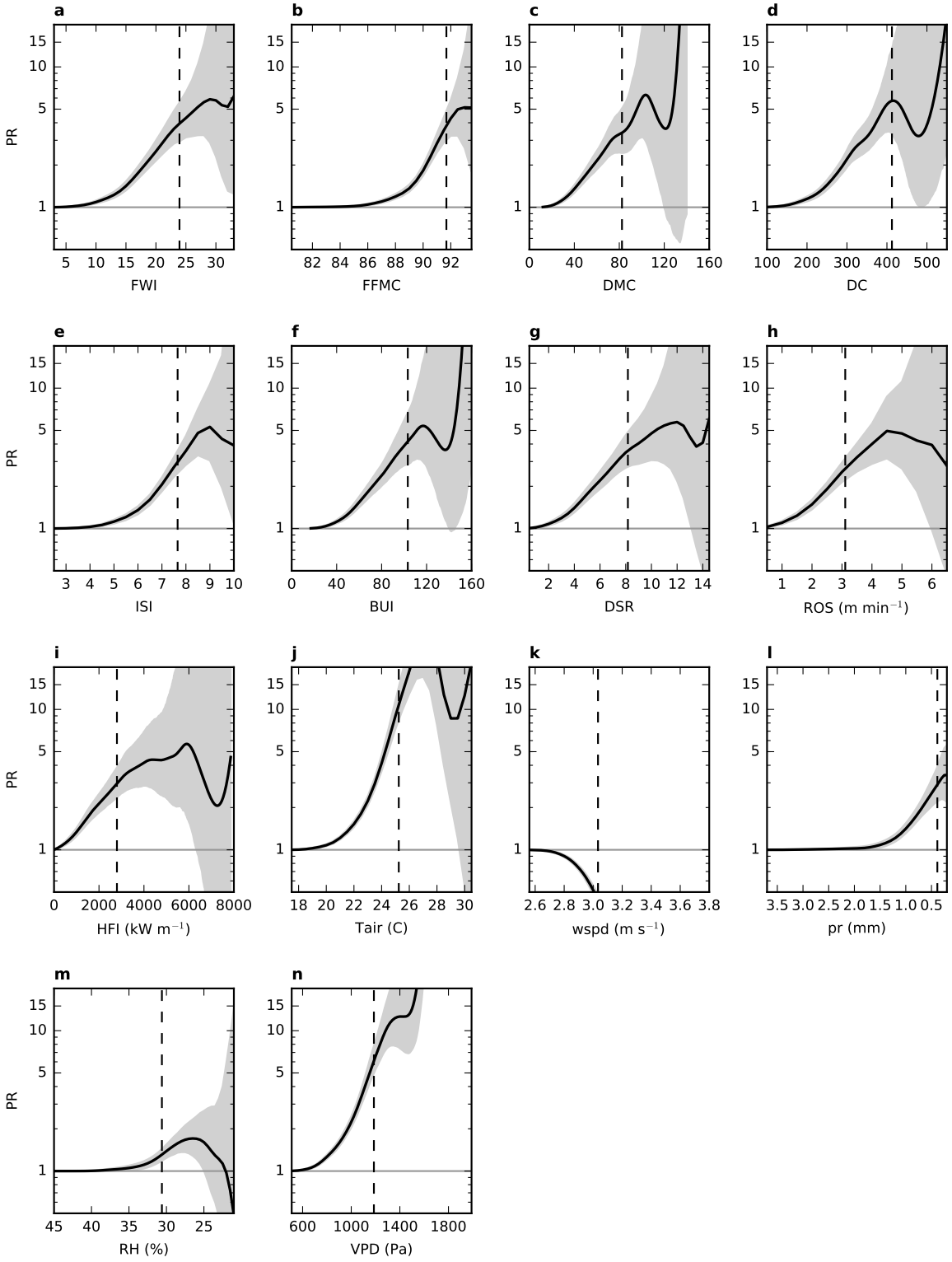

Figure S5: As in Fig. S4 but for PR. Note the vertical axis uses a log scale.

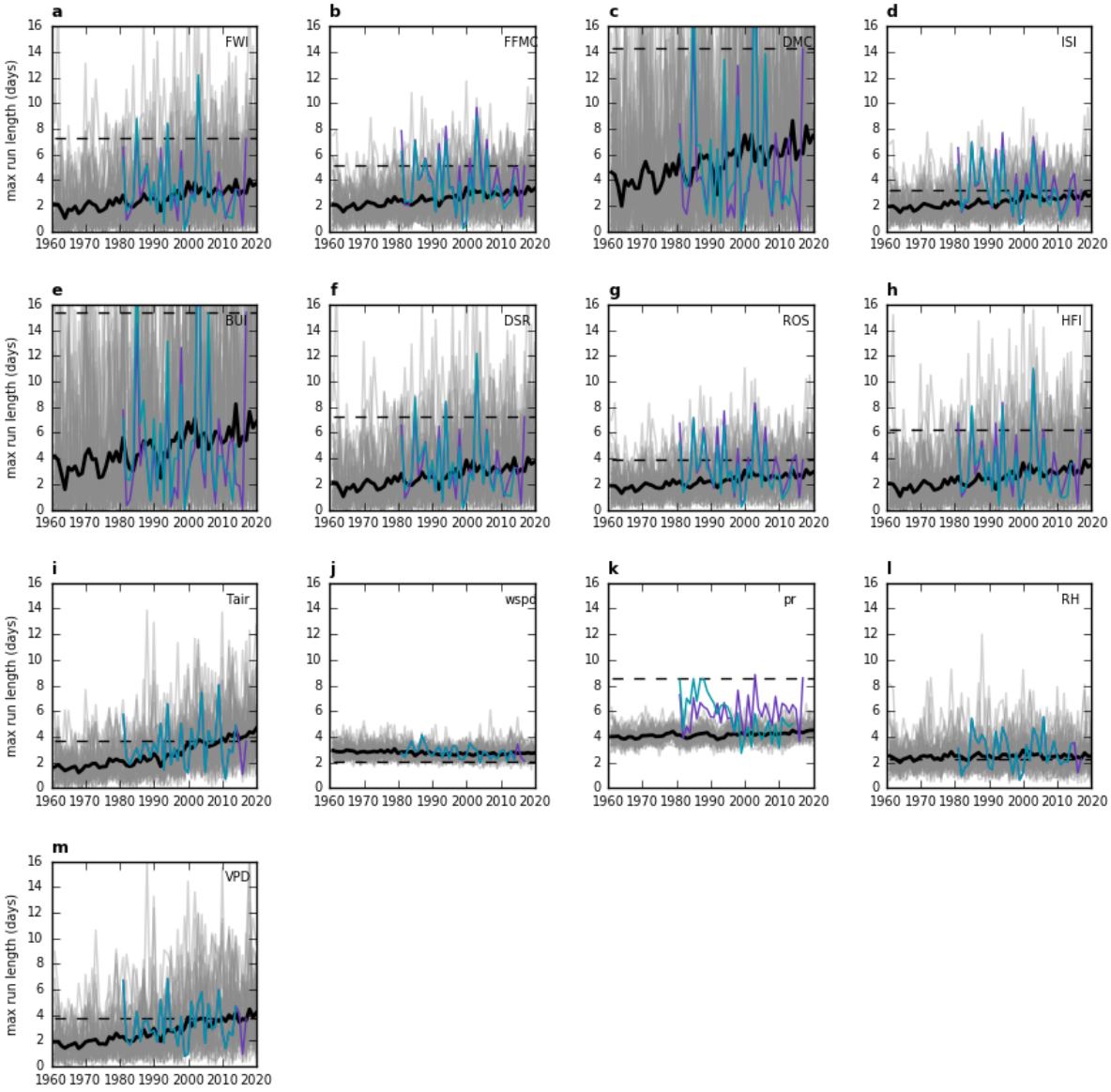

Figure S6: Similar to Fig. S3 but plotting the length of the maximum number of consecutive days during the fire season that exceed the climatological 90th percentile value for each CFFDRS index and input variable noted in the top right of each subplot. DC is excluded because it tends to increase through the fire season (Amiro et al., 2004).

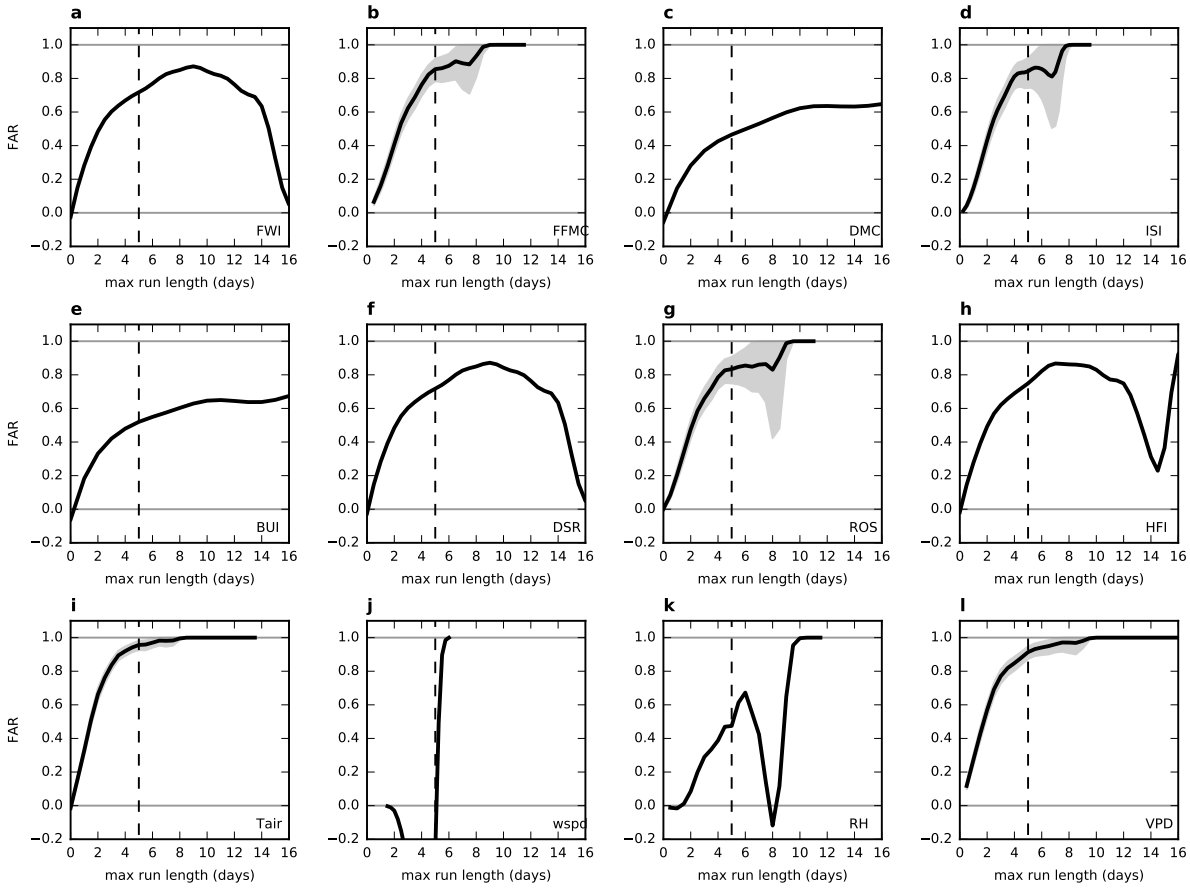

Figure S7: As in Fig. S4 but for a maximum run length exceeding the threshold on the horizontal axis. A run is defined by consecutive days during the fire season exceeding the climatological 90th percentile value for each CFFDRS index and input variable noted in the top right of each subplot.

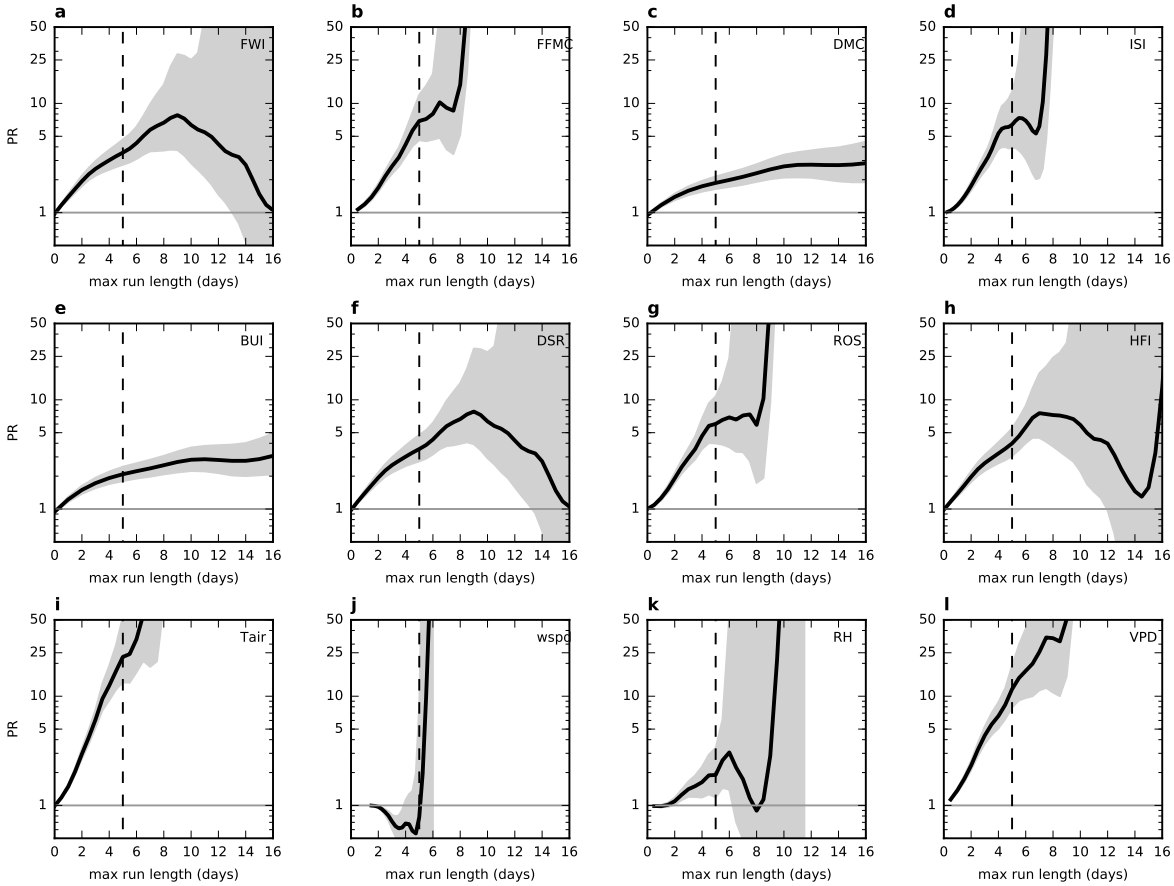

Figure S8: As in Fig. S5 but for a maximum run length exceeding the threshold on the horizontal axis. A run is defined by consecutive days during the fire season exceeding the climatological 90th percentile value for each CFFDRS index and input variable noted in the bottom right of each subplot. Note the vertical axis uses a log scale.

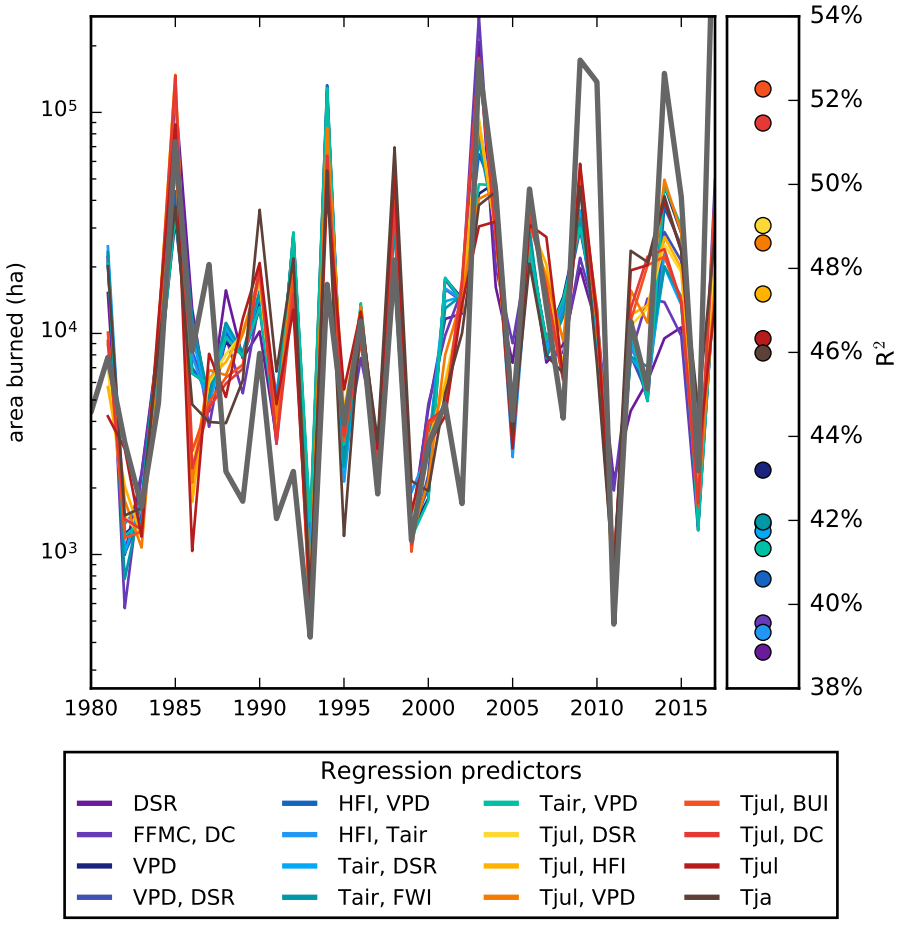

Figure S9: Area burned from observations (grey dashed line) and predicted from a linear regression model using different predictor sets (colors) from the MERRA2/MSWEP dataset. Area burned in ha is plotted on a log scale. The right panel displays the variance explained for each regression using a cross-validation. Predictors refer to the 95th percentile values used in the event attribution analysis, except for the temperatures averaged over July (Tjul) and July-August (Tja).

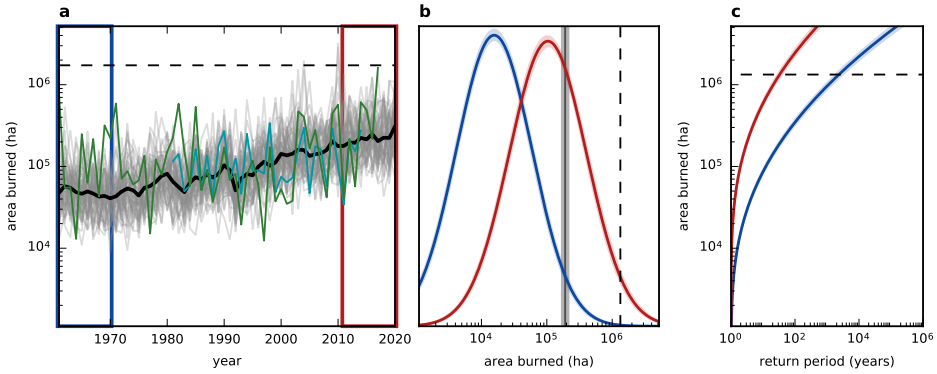

Figure S10: Time series (a, log scale) of regression-predicted annual burned area in BC for CanRCM4 realizations (grey) pre-bias correction and ensemble mean (bold), reanalysis (turquoise), and observations (green). The dashed line marks the observed 2017 value. Probability distributions (b) for area burned amounts (log scale) from decades outlined in corresponding colors in (a). The grey bar indicates the area burned amount in the distribution with reduced anthropogenic influence (blue) of a corresponding percentile to the 2017 amount (dashed line) in the distribution of the current decade, which includes anthropogenic influence (red). The distributions in (b) are used to derive return periods in years for area burned amounts (c). The regression model uses July mean temperature as a predictor, with shading in (b) and (c) demonstrating the 90% confidence interval.

Table S1: List of CFFDRS indices and input variables. Adapted from Kirchmeier-Young et al. (2017); see Wotton (2009) for more detail.

CFFDRS Index	Abbreviation	Description
Fire Weather Index	FWI	Summary of fire potential
Fine Fuels Moisture Code	FFMC	Moisture in surface fuels
Duff Moisture Code	DMC	Moisture in decaying litter and upper layers
Drought Code	DC	Moisture in deep layers and large debris
Initial Spread Index	ISI	Potential fire spread
Build-up Index	BUI	Summary of available fuels
Daily Severity Rating	DSR	Rescaled FWI for categorical interpretation
Rate of Spread	ROS	Rate [m min^{-1}] at which the fire head (leading edge) moves
Head Fire Intensity	HFI	Intensity [kW m^{-1}] at the fire head
Air temperature	Tair	Local-noon air temperature [C]
Relative humidity	RH	Local-noon relative humidity [%]
Wind speed	wspd	Local-noon wind speed [m s^{-1}]
Precipitation	pr	24-hour accumulated precipitation at local noon [mm]
Vapor pressure deficit	VPD	Daily vapor pressure deficit [Pa]

Table S2: List of R^2, RMSE, and AIC for the tested regression models for the natural log of annual area burned, using cross-validation. For the right three columns, the predictors and predictand have first had a linear trend removed. As in Fig. S9, predictors refer to the 95th percentile values used in the event attribution analysis, except for the temperatures averaged over July (Tjul) and July-August (Tja).

	Original			Detrended		
Predictors	R^2	RMSE	AIC	R^2	RMSE	AIC
DSR	0.39	1.26	118.4	0.45	1.14	111.4
FFMC, DMC	0.39	1.26	120.2	0.43	1.17	115.0
VPD	0.47	1.17	113.3	0.46	1.13	111.0
VPD, DSR	0.45	1.20	116.7	0.46	1.12	112.5
HFI, VPD	0.43	1.22	117.8	0.45	1.14	113.6
Tair, HFI	0.44	1.21	117.5	0.47	1.12	112.0
Tair, DSR	0.45	1.20	116.6	0.49	1.10	111.1
Tair, FWI	0.45	1.20	116.9	0.48	1.11	111.4
Tair, VPD	0.44	1.21	117.3	0.43	1.16	114.9
Tjul, DSR	0.56	1.07	109.2	0.56	1.02	106.1
Tjul, HFI	0.55	1.08	110.0	0.55	1.04	106.9
Tjul, VPD	0.55	1.08	109.9	0.52	1.07	108.8
Tjul, BUI	0.58	1.05	107.9	0.57	1.01	105.2
Tjul, DMC	0.55	1.08	109.7	0.55	1.04	106.9
Tjul	0.54	1.10	108.9	0.50	1.08	107.8
Tja	0.47	1.17	113.2	0.45	1.14	111.5